Polarization Characteristics of Spectralon Illuminated by Coherent Light

David A. Haner, Brendan T. McGuckin, and Carol J. Bruegge

Abstract - **The Multi-angle Imaging SpectroRadiometer (MISR) makes use of an on-board calibration system to provide routine absolute radiometric calibrations of the instrument while in flight. In addition to on-board detector standards, two Spectralon panels will reflect sunlight into the nine cameras. Prior to assembling the instrument, these panels were quantified in terms of their bidirectional reflectance distribution function (BRDF). Included in the testing were principal-plane measurements where polarizations of the source and detector were analyzed. The BRDF was measured as a function of the detector angle over an elevation range of 0° to 85°, in 5° increments, as referenced from the panel normal. This was done at laser wavelengths of 442.0, 632.8, and 859.9 nm. The BRDF was found to increase in the forward direction, at all wavelengths, for both an increasing angle of incidence and angle of reflection. This forward-scattering effect is greater for the incident perpendicular, s-polarization state than for the parallel, p-polarization state. Conversely, the incident parallel state has a larger BRDF than the perpendicular polarization state at the larger backward scattering angles.The fraction of polarization is reported here for these cases.**

Index Terms - **Reflectance standards, Spectralon, polarization**

D.A. Haner is with the Department of Chemistry, California State Polytechnic University, Pomona, Pomona, CA 91768 USA.

B.T. McGuckin is Director of Capital City Lasers, P.O. Box 13047, 17 Research Ave., Heriot Watt Research Park, South Edinburgh, EH14-4YG, U.K.

C.J. Bruegge is with the Jet Propulsion Laboratory, California Institute of Technology, 4800 Oak Grove Drive, Pasadena, CA 91109 USA (Carol.Bruegge@Jpl.Nasa.Gov).

IEEE TRANSACTIONS ON GEOSCIENCE AND REMOTE SENSING. DRAFT DATE FEBRUARY 25, 1999.

I. INTRODUCTION

The utilization of On-Board Calibrator (OBC) systems on satellite remote sensors has stimulated interest in materials for diffuse reflectance standards. For example, the Sea Viewing Wide Field Sensor (SeaWiFS) includes a diffuse panel made of white thermal control paint YB71. An alternative OBC material is Spectralon, a pure sintered polytetrafluoroethylene (PTFE) type material supplied by Labsphere, Inc. It has been the favored choice for use on the Multi-angle Imaging SpectroRadiometer (MISR), which belongs to the suite of NASA Earth Observing System (EOS) sensors. The MISR program elected Spectralon because of its brightness and diffuse properties, and was the first to flight qualify the material for satellite remote sensing [1]. Two Spectralon panels, together with their associated deploying mechanisms and calibration diodes, constitute the OBC system for MISR [2]. The diffuse panels will be deployed at monthly intervals, over the poles, to reflect solar irradiance into each of the "pushbroom" camera banks. When not is use they will be stowed and protected.

In preparation for their deployment on MISR, a number of Spectralon panels have undergone an extensive series of pre-flight tests of the optical reflectance characteristics [3]. For ease of comprehensive testing, 4" square test pieces were often measured, rather than the 3" x 25" flight panels. These pieces were made from the same molding runs as their flight counterparts. Experiments have established the correlation between the reflectance of the test pieces and the flight panels to within ~0.4%. This included comparisons over a large range of experimental conditions and polarization combinations. This agreement gives confidence that the polarization characteristics made with a given test piece can be generally transferred to the larger calibration panels.

While it has been established that the MISR cameras are not polarization sensitive, knowledge of the polarization of light is desirable for modeling of the panel response. Other applications for these data are experiments where panel-incident sunlight has first traversed the Earth's atmosphere or limb, and has become partially polarized in consequence of the atmospheric scattering processes. Likewise, should the detection system have polarization sensitivity, the polarization properties of the atmosphere and panel would need to be known.

The objective of this experiment was to measure the BRDF under both polarized and unpolarized illumination conditions. The latter was estimated by making linear combination of data acquired using polarized light. Required for this study was a variably polarized source, and an ability to make absolute scale measurements. The results of this study are presented here. We begin, however, by first presenting an overview of the BRDF parameters and nomenclature that will be used throughout this text.

II. NOMENCLATURE

In the following we refer to p- and s-polarized states. By this we mean the electric field vector is orientated in the parallel, or perpendicular direction, respectively. This is relative to the principal plane containing the diffuse-panel normal, the incident wave-vector, and the detector view axis.

A. BRDF nomenclature for polarized geometries

The bi-directional reflectance distribution function (BRDF) is the invariant quantity which characterizes the geometrical reflecting property of a reflecting surface. The BRDF is to be defined for a particular wavelength and polarization of the incident and reflected beams. It will depend upon the spectroscopic properties of the material, as well as the physical properties of the surface. Our BRDF notation is expanded from that given in by Nicodimus, et. al. [5]:

$$f_{ir}(\theta_i,\varphi_i;\theta_r,\varphi_r;\lambda) = \frac{dL_r(\theta_i,\varphi_i;\theta_r,\varphi_r;E_i;\lambda)}{dE_i(\theta_i,\varphi_i;\lambda)} \quad . \tag{1}$$

where

f_{ir} is the BRDF for i-incident and r-detected polarization

dL_r is the radiance observed by a detector

E_i defines the incident polarization state, with dE_i the magnitude

θ_i is the incident elevation angle with respect to the panel normal

ϕ_i is the detector azimuth angle, defined as 0°

θ_r is the detector elevation angle with respect to the panel normal (set negative for backward scattering)

ϕ_r is the detector azimuthal angle (defined as 0° for backscattered light)

λ is the wavelength of irradiance

Two subscripts are used to denote the incident and reflected polarization states, respectively. Each subscript may take on a value of s, p, or u. As an example, sp would indicate that the incident polarization is s, and that the detected component is of p-polarization. The subscript u may also be used, to denote an unpolarized source, or a detection that includes measurement of the total reflected radiance, irrespective of polarization state. The variable λ is equal to the wavelength at which the measurement is made.

By assuming an unpolarized source, and by selectively measuring each of the reflected orthogonal polarization components in turn, the BRDF for a polarization-insensitive detector can be determined:

$$f_{uu}(\theta_i,\varphi_i;\theta_r,\varphi_r;\lambda) = \frac{dL_s(\theta_i,\varphi_i;\theta_r,\varphi_r;E_u;\lambda)}{dE_u(\theta_i,\varphi_i;\lambda)} + \frac{dL_p(\theta_i,\varphi_i;\theta_r,\varphi_r;E_u;\lambda)}{dE_u(\theta_i,\varphi_i;\lambda)} \tag{2}$$

This, expressed in shorthand notation, is $f_{uu} = f_{us} + f_{up} = 1/\pi$ (ideal). The relationship represented by the first equal sign is true in general. The relationship qualified with the notation "ideal" is true only for a diffuse reflector that is perfectly lambertian. Of course no such reflector exists in practice, but it will be useful to compare our panels to this ideal case. For the ideal diffuse reflector, each detected component has a BRDF equal to $1/2\pi$ (or 0.159), with the unpolarized reflected beam equal to $1/\pi$, irrespective of view angle.

We can further explore each of the above terms by dividing this unpolarized source beam into two equal, orthogonally-polarized components of magnitude:

$$dE_u(\theta_i,\phi_i;\lambda) = 2dE_s(\theta_i,\phi_i;\lambda) = 2dE_p(\theta_i,\phi_i;\lambda)\ . \tag{3}$$

The BRDF for each of the detected components can now be found:

$$f_{us}(\theta_i,\varphi_i;\theta_r,\varphi_r;\lambda) = \frac{dL_s(\theta_i,\varphi_i;\theta_r,\varphi_r;E_s;\lambda)}{2dE_s(\theta_i,\varphi_i;\lambda)} + \frac{dL_p(\theta_i,\varphi_i;\theta_r,\varphi_r;E_p;\lambda)}{2dE_p(\theta_i,\varphi_i;\lambda)}\ . \tag{4}$$

In our shorthand notation this gives $f_{us} = (f_{ss} + f_{ps})/\,2 = 1/2\pi$ (ideal). We would similarly write $f_{up} = (f_{sp} + f_{pp})/\,2 = 1/2\pi$ (ideal). Combining each of these with Eqn. 2 we write $f_{uu} = (f_{ss} + f_{ps} + f_{sp} + f_{pp})/2 = 1/\pi$ (ideal) .

For the case of a polarized source and the unpolarized detector, the BRDF can be broken into two terms for the orthogonal components at the detector. Considering a s-polarized source we arrive at:

$$f_{su}(\theta_i,\varphi_i;\theta_r,\varphi_r;\lambda) = \frac{dL_s(\theta_i,\varphi_i;\theta_r,\varphi_r;E_s;\lambda)}{dE_s(\theta_i,\varphi_i;\lambda)} + \frac{dL_p(\theta_i,\varphi_i;\theta_r,\varphi_r;E_s;\lambda)}{dE_s(\theta_i,\varphi_i;\lambda)} \quad . \tag{5}$$

In abbreviation this gives $f_{su} = f_{ss} + f_{sp} = 1/\pi$ (ideal). Likewise, $f_{pu} = p_{ss} + f_{pp} = 1/\pi$ (ideal) .

In a subsequent section we will use these relationships to find the various BRDF parameters we wish to report.That is, the results of these data computations are presented as the polarized components of the BRDF: f_{ss}, f_{sp}, f_{pp}, and f_{ps} .

B. Fraction of polarization

In addition to the BRDF retrievals, it is interesting to describe the reflected beam with regards to the degree in which it is polarized. We therefore report the fraction of polarization [7] for either the s- or p-incident light:

$$P_s = \frac{f_{ss} - f_{sp}}{f_{ss} + f_{sp}} \text{ and } P_p = \frac{f_{pp} - f_{ps}}{f_{pp} + f_{ps}} \quad . \tag{6}$$

Combining all calibrated polarization data at a single angle of incidence and for a particular wavelength produces an estimate of the fraction of polarization for an unpolarized source:

$$P_u = \frac{(f_{ss} + f_{ps}) - (f_{pp} + f_{ps})}{f_{ss} + f_{sp} + f_{pp} + f_{ps}} \tag{7}$$

Combining all calibrated polarization data at a single angle of incidence and for a particular wavelength produces an estimate of the fraction of polarization for an unpolarized source:

$$P_u = \frac{(f_{ss} + f_{ps}) - (f_{pp} + f_{ps})}{f_{ss} + f_{sp} + f_{pp} + f_{ps}} \tag{8}$$

The first factor is the s-detected component for an unpolarized source; the second factor is the p-detected component for an unpolarized source.

III. EXPERIMENTAL SET-UP

The hardware for this experiment is similar to that described elsewhere in great detail [4], and is shown here by the schematic in Fig. 1. Three lasers were collimated and made to selectively impinge on the target. The target, in turn, was attached to rotation stages and to the bed of a ±45° goniometric cradle. In all, three computerized positioners allowed the target to be orientated with respect to the incident beam. A detector was additionally rotated about a common vertical axis. These allowed us to measure the BRDF at several illumination geometries, for a complete mesh of points over the view hemisphere, and for multiple wavelengths.

In order to reduce the effect of minor power fluctuations, the detection system was composed of two identical telescopes: one for measurement of the panel-reflected light, and the other for illumination stability monitoring. The signals from both detectors were phase detected in synchronization with the chopped beam, and then ratio recorded, digitized, and stored in computer data files. The three wavelengths utilized were chosen for their proximity to MISR spectral bands. Lasers were utilized so that high signal-to-noise detection could be achieved. These were helium cadmium (HeCd), lasing at 442.0 nm, a helium neon (HeNe) laser at 632.8

nm, and a GaAlAs semiconductor diode laser source, at 859.9 nm. A second half-waveplate, of zero order, was used at each wavelength to set the incident-beam polarization to either the p- or s-polarized states. These states have the electric field vector parallel and perpendicular, respectively, relative to the principal plane containing the Spectralon normal. Also utilized was a 500:1 extinction ratio polarizer cube, mounted to a rotation stage and located immediately in front of the detector telescope assembly used to view the panel-scattered light. The cube's aperture was sufficiently large to avoid compromising the 2° angular resolution of the telescope. Polarizer rotation by 90° between data runs permitted resolution of the scattered light into its orthogonally-polarized components, each of which was measured sequentially.

The experimental data was converted from the digitized voltages to BRDF using the following algorithm [6]:

$$f_{ir}(\theta_i,\varphi_i;\theta_r,\varphi_r;\lambda) = \frac{[(V_r(\theta_i,\varphi_i;\theta_r,\varphi_r;E_s;\lambda))/V_{ref}]/\Omega_d \cos\theta_r}{[V_{i,\,filter}/V_{ref}]\cdot 10^{ND}} \tag{9}$$

where

V_r/V_{ref} is the digitized detector voltage ratioed to the reference beam voltage

Ω_d is the solid angle of detector

$V_{i,filter}/V_{ref}$ is the voltage obtained when viewing the incident beam through the neutral-density filter and as ratioed to the reference beam voltage, and

ND is the filter neutral density value applicable when directly viewing the incident beam.

IV. RESULTS AND DISCUSSION

The results shown here are from our test sample number 12969, position 1. Although in general we found our samples to be spatially homogeneous, position 1 was noted to have a slight depression. (All data required for our flight program were retaken at position 2 [3]).

The data is presented in graphic form. The break in the curves is at a view angle which was obstructed by the incident beam. The dotted line at 0.159 (equal to $1/2\pi$) represents the value expected for an ideal diffuser, and is given as reference. Note that the ordinate scales change with the incident angles, but are uniform over the wavelengths.

Figures 2, 4, and 6 will each show the four polarized components of the BRDF (distinguished as four curves within a plot window). This is done at wavelengths 442.0, 632,8, and 859.9 nm, respectively for the three figures. Other dependencies studied are incident angle (figures a-d), and detector view angle (x-axes values). Figures 3, 5, and 7 will show the fraction of polarization for the s- and p-incident polarizations and for the unpolarized source. They are likewise given as a function of wavelength, incident angles, and detector view angle.

Spectralon is non-absorbing at our wavelengths, and multiple scattering is so efficient that no appreciable light is transmitted if the thickness is greater than 6.0 mm. The directional-hemispherical reflectance has been measured to be ≅ 0.99 [6]. The polarization properties of Spectralon at 442.0, 632.8, and 859.9 nm are in general very similar. These general features will be discussed in detail using the complete spectrum of measurements at 859.9 nm.

The first reflectance feature to be noted is that there is no discernible specular reflection from the surface under any experimental conditions. This result proves that the surface is not continuous in the usual sense. However, there is a retroreflectance peak, of the same polarization as the incident light, that is 8.0% above the diffuse reflectance. This peak seems to rise and fall completely within 15° at normal incidence. Since there is no retroreflectance in the polarization orthogonal to the incident polarization, the retroreflectance is a small surface effect with a probable mechanism of shadow hiding [8].

Figure 6a shows all four polarized components of BRDF for normal incidence where the ss (solid line) and pp ("x" symbols) components are nearly the same magnitude, and are roughly 12% greater than the sp (dashed line) and ps ("+" symbols) components. Thus it appears that there is a higher reflectance where there is "no change" in the state of polarization. However, the fact that the components with "opposite" polarization (i.e., the sp and ps cases) also have a large magnitude indicates that the material is an excellent diffuse reflector. For these cases the BRDF are nearly equal to the ideal reflector value. (The ideal value of 0.159 is shown by the dashed line). Conversely, there is evidence that while the material is diffuse, it is not perfectly lambertian. For example, the BRDF profiles are decreasing as the detector moves from the surface normal, rather than remain constant. It is noted that the measurement of BRDF is greater than the ideal diffuse reflector at angles near the surface normal, and less than the ideal reflector at large angles from the normal.

At 30° incidence, shown in Fig. 6b, the magnitude of the opposite polarization components of BRDF remain nearly the same as their values at 0° incidence. This constancy is to be expected as these components are the result of the efficient depolarization of incident light by the diffuse reflectance (due to multiple scattering in the volume). The curves which depict the no-change components are found to increase in magnitude, with the ss component being larger than the pp as the forward scattering angle increases. The ss BRDF component is seen to increase monotonically from the back scattering angles to the maximum forward scattering angle. This distribution would correspond to scattering from a surface composed of randomly oriented facets where the s polarization would dominate in the forward direction since it is more efficiently reflected [9, 10]. In direct contrast, in the backward scattering angles the pp component is greater than the ss component. The detector angle at which these components are equal is about -20 degrees (we denote this as the "cross-over" angle). This can be explained by recalling that classically the p -polarized incident light is preferentially transmitted into the material, with less light reflected in the forward direction. This suggests that the p-polarized irradiance will contribute most efficiently to the multiple scattering, which is depolarizing.

At 45° incidence, shown in Fig. 6c, the polarized BRDF profiles for the no-change polarization cases increase in magnitude in the forward direction, however there is only slight change in magnitude in the backward angles. The oppositely polarized BRDF components remain unchanged in magnitude and shape. As the angle of incidence is increased to 60°, shown in Fig. 6d, there are direct increases in the same polarization components where ss > pp > sp ≅ ps in the forward scattering angles, and pp > ss > sp ≅ ps in the backward scattering angles, and the cross-over angles appears to remain fixed at $\theta_r = -20°$.

Figure 7a shows all the fractions of polarization, P_p (dashed line), P_s (solid line), and P_u ("+" symbols), calculated from the polarized components of BRDF as a function of the view angle, for illumination along the panel normal, $\theta_i = 0°$. P_s and P_p are nearly the same shape and magnitude as a function of view angle and have a small positive magnitude of about 0.03. P_u is nearly constant for this illumination case and for all view angles, which would be expected for bulk-scattering reflectors. One final note is that fraction of polarization at the large angles of reflection show large variations. This is due to the subtraction of small numbers which enhances the experimental noise.

As the angle of incidence increases to 30°, see Fig. 7b, the fractions of polarization all increase monotonically in the forward direction. P_s has the greatest value and decreases uniformly in the backward scattering angles. P_p appears to have a point of inflection at $\theta_r = 0°$, and increases with negative curvature in the backward scattering angles. P_u generally increases with increasing view angle, and has an inversion angle at $\theta_r = -10°$ where the fraction of polarization becomes negative. Negative polarization is a recognized property of materials characterized as volume or diffuse scatterers [11]. The inversion angle occurs when the fraction of polarization for P_s and P_p are equal and becomes negative when $P_p > P_s$. Further increases in the angle of incidence to 45° and 60°, see Fig. 7c and 7d, show an increase the magnitude of the fractions of polarization. We also see that their general functional behavior remains the same.

The fraction of polarization for an unpolarized source, P_u, at the greatest backward scattering angle is nearly constant in magnitude for all angles of incidence. It is an increasing function of incidence angle in the forward scattering direction.

There are certain features in the polarized components of the BRDF which are functions of wavelength of the incident irradiance. These are shown by reference to Figs. 2 and 3, at a wavelength of 442.0 nm, and Figs. 4 and 5, for 632.8 nm. The most noticeable contrast for the incident wavelength is seen in Figs. 3a, 5a, 7a where it is seen that the fraction of polarization for the p-incident polarization has a greater magnitude than the fraction polarization for the s-incident polarization . This would not be expected, since at 0° the plane of incidence is not defined. This difference in fraction of polarization decreases with the longer wavelengths. Additionally, variability in the BRDF with spatial location becomes more pronounced at shorter wavelengths [12]. These features were small, about 2%, and on the same order as the variability noticed for these polarization studies. One final wavelength-dependent variability is the slight difference in the position of the inversion angles. These effects are attributed to surface roughness resulting from the manufacturing process. Surface figuring could accentuate one polarization of the beam over the other, and shows the potential importance of the mechanical properties of the reflecting surface which can modulate the BRDF as a function of sample orientation as well as wavelength.

V. CONCLUSIONS

Reflectance from Spectralon is a combination of a diffuse component, due to internal scattering, and an off-specular component due to reflection from the surface facets. The effect of the latter are more evident at large angles of incidence and reflection.

The polarization of light from a Spectralon test piece has been made for both s-and p-polarized incident light. This was done at 442.0, 632.8, and 859.9 nm, at 0°, 30°, 45°, and 60° angles of incident, and for view angles ranging from 0° to 85° in 5° steps. It is shown that for the forward scatter direction, BRDF increases with view angle.

These data will enable those who choose Spectralon for the calibration of flight instruments to accurately model the instrument response when polarized light is incident on the panels, or if the detectors are polarization sensitive and the incident light is unpolarized. The results of these measurements are qualitatively consistent with the results of earlier and recent researchers [12, 13].

An estimator of the fraction of polarization of the reflected light for an unpolarized source has been presented here, using polarized lasers. As round-robin comparisons of our data have shown agreement to within ±0.5% in BRDF [14], we feel confident that such laser-based methodologies do provide accurate representations of unpolarized, incoherent illumination results.

ACKNOWLEDGMENTS

This work was carried out at the Jet Propulsion Laboratory, California Institute of Technology, under contract with the National Aeronautics and Space Administration (NASA). The authors acknowledge the technical support of S. Dermenjian, C. Esproles and A. Brothers and also valuable discussions with R. T. Menzies, and V. Duval.

REFERENCES

[1] C. J. Bruegge, A. E. Steigman, R. A. Rainen and A. W. Springstein, "Use of Spectralon as a diffuse reflectance standard for in-flight calibration of earth-orbiting sensors," Opt. Eng., Vol. 32, No. 4, pp 805-814, Apr. 1993.

[2] C. J. Bruegge, V. G. Duval, N. L. Chrien and D. J. Diner, "Calibration plans for the Multi-angle Imaging SpectroRadiometer (MISR)," Metrologia, Vol. 30, No. 4, pp 213-221, Oct. 1993.

[3] C.J Bruegge, N.L. Chrien, D.A. Haner," A Spectralon BRF data base for MISR calibration applications," submitted to Remote Sensing Of Environment, 1998.

[4] B. T. McGuckin, D. A. Haner, R. T. Menzies, C. Esproles and A. M. Brothers, "Directional reflectance characterization facility and measurement methodology, Appl. Opt., Vol. 35, No. 24, pp. 4827- 4834, Aug. 1996.

[5] F. E. Nicodimus, J. C. Richmmond, J. J. Hsia, I. W. Ginsburg, and T. Limperis, "Geometrical considerations and nomenclature for reflectance," Natl. Burl Stand. (U. S.) Monogr. 160, 1977.

[6] D. A. Haner, B. T. McGuckin, R. T. Menzies, C. J. Bruegge, and V. Duval, " Directional-hemispherical reflectance for Spectralon by integration of its bi-directional reflectance," Appl. Opt., Vol. 37, No. 18, pp 3996-3999, June 1998.

[7] W. G. Egan, J. Grusauskas, and H. B. Hallock, "Optical depolarization properties of surfaces illuminated by coherent light," Appl. Opt., Vol. 7, No. 8, pp 1529-1534, Aug. 1968.

[8] D. A. Haner and R. T. Menzies, "Reflectance characteristics of reflectance materials used in lidar hard target calibration," Appl. Opt., Vol. 28, No. 5, pp 857-864, Mar. 1989.

[9] K .E. Torrance, E. M. Sparrow and R. C. Birkebak, "Polarization, directional distribution, and off-Specular phenomena in light reflected from roughened surfaces," J. Opt. Soc . Am., Vol. 56, No. 7, pp 916-925, July 1966.

[10] K. E. Torrance, "Theoretical polarization of off-specular reflection peaks," J. Heat Transfer, Vol. 91, No. 2, pp 287-290, May 1969.

[11] D. C. Cramer and M. E. Blair, "Some polarization characteristics of magnesium oxide and other diffuse reflectors," Appl. Opt., Vol. 8, No. 8, pp 1597-1605, Aug. 1969.

[12] B. T. McGuckin, D. A. Haner and R. T. Menzies, "Multi-angle Imaging SpectroRadiometer: optical characterization of the calibration panels", Appl. Opt., Vol. 36, No. 27, pp 7016-7022, Sept. 1997.

[13] G. C. McCoyd, "Polarization properties of a simple dielectric rough surface model," J. Opt. Soc. Am., Vol. 57, No. 11, pp 1345-1350, Nov. 1967.

[14] E. A. Early, P. Y. Barnes, B. C. Johnson, J. J. Butler, C. J. Bruegge, F. Biggar, P. R. Syak, M. M. Pavlov," Bi-directional reflectance round robin in support of the Earth Observing System program", submitted to J. Atmos. and Oceanic Technology, 1998.

FIGURE CAPTIONS

Figure 1. Optical Setup, where s is the reflecting surface, d the polarization sensitive detector, and B the polarized incident beam. Subscript i is used for the incident angles, and r is used for the reflecting angles. The z axis is coincident with the surface normal, θ is the elevation angle with respect to the surface normal, and ϕ is the azimuthal angle defined with respect to the incident beam.

Figure 2. Bi-directional reflectance distribution function as a function of polarization at 442.0 nm for a range of detector angles. Negative values correspond to backward scattering angles, $\phi_r = 0°$, where: — $= f_{ss}$, ---- $= f_{sp}$, xxx $= f_{pp}$, +++ $= f_{ps}$, and . . . $= f_{ideal}$.

Figure 3. Fraction polarization at 442.0 nm. as a function of the detector angle. Negative values correspond to backward scattering angles, $\phi_r = 0°$, — $= P_s$ ----- $= P_p$, +++ $= P_u$.

Figure 4. Bi-directional reflectance distribution function as a function of polarization at 632.8 nm for a range of detector angles. Negative values correspond to backward scattering angles, where: — $= f_{ss}$, ---- $= f_{sp}$, xxx $= f_{pp}$, +++ $= f_{ps}$, and . . . $= f_{ideal}$.

Figure 5. Fraction polarization at 632.8 nm. as a function of the detector angle. Negative values correspond to backward scattering angles, $\phi_r = 0°$, — $= P_s$ ----- $= P_p$, +++ $= P_u$.

Figure 6. Bi-directional reflectance distribution function as a function of polarization at 859.9 nm for a range of detector angles. Negative values correspond to backward scattering angles, where: — $= f_{ss}$, ---- $= f_{sp}$, xxx $= f_{pp}$, +++ $= f_{ps}$, and . . . $= f_{ideal}$.

Figure 7. Fraction polarization at 859.9 nm. as a function of the detector angle. Negative values correspond to backward scattering angles, $\phi_r = 0°$, — $= P_s$ ----- $= P_p$, +++ $= P_u$.

BIOGRAPHIES

David A. Haner

Brendan McGuckin

Carol J. (Kastner) Bruegge received BA and MS degrees in Applied Physics at the University of California, San Diego, in 1978, and MS and Ph.D. degrees in Optical Sciences at the University of Arizona, Tucson, in 1985. Her experience is in the areas of terrestrial remote sensing, calibration of remote sensing sensors, radiative transfer, and use of ground-truth measurements for validation and calibration of airborne or in-orbit sensors and sensor data. Presently employed by JPL, she serves as the Instrument Scientist for the Earth Observing System (EOS)/ Multi-angle Imaging SpectroRadiometer (MISR). Additionally, she has provided support in the absolute radiometric calibration of the Landsat Thematic Mapper, and other airborne and spaceborne instruments. She has been a Principal Investigator in the First International Satellite Land Surface Climatology Program (ISLSCP) Field Experiment (FIFE), a ground-truth hydrology experiment conducted from 1987 through 1989.

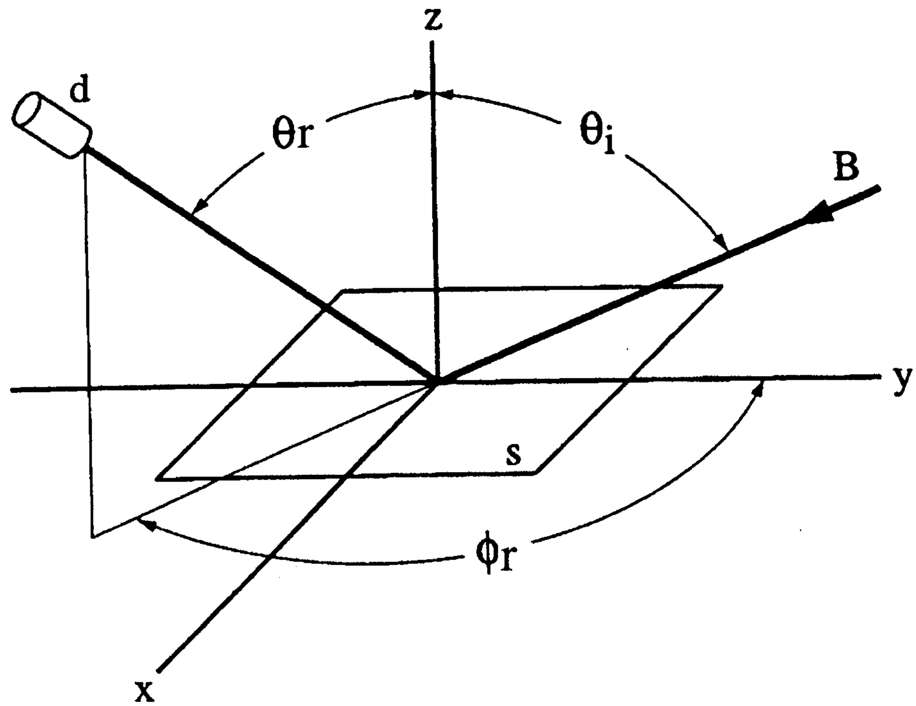
z
d
θr
θi
B
y
s
φr
x

FIGURE 2
HANER

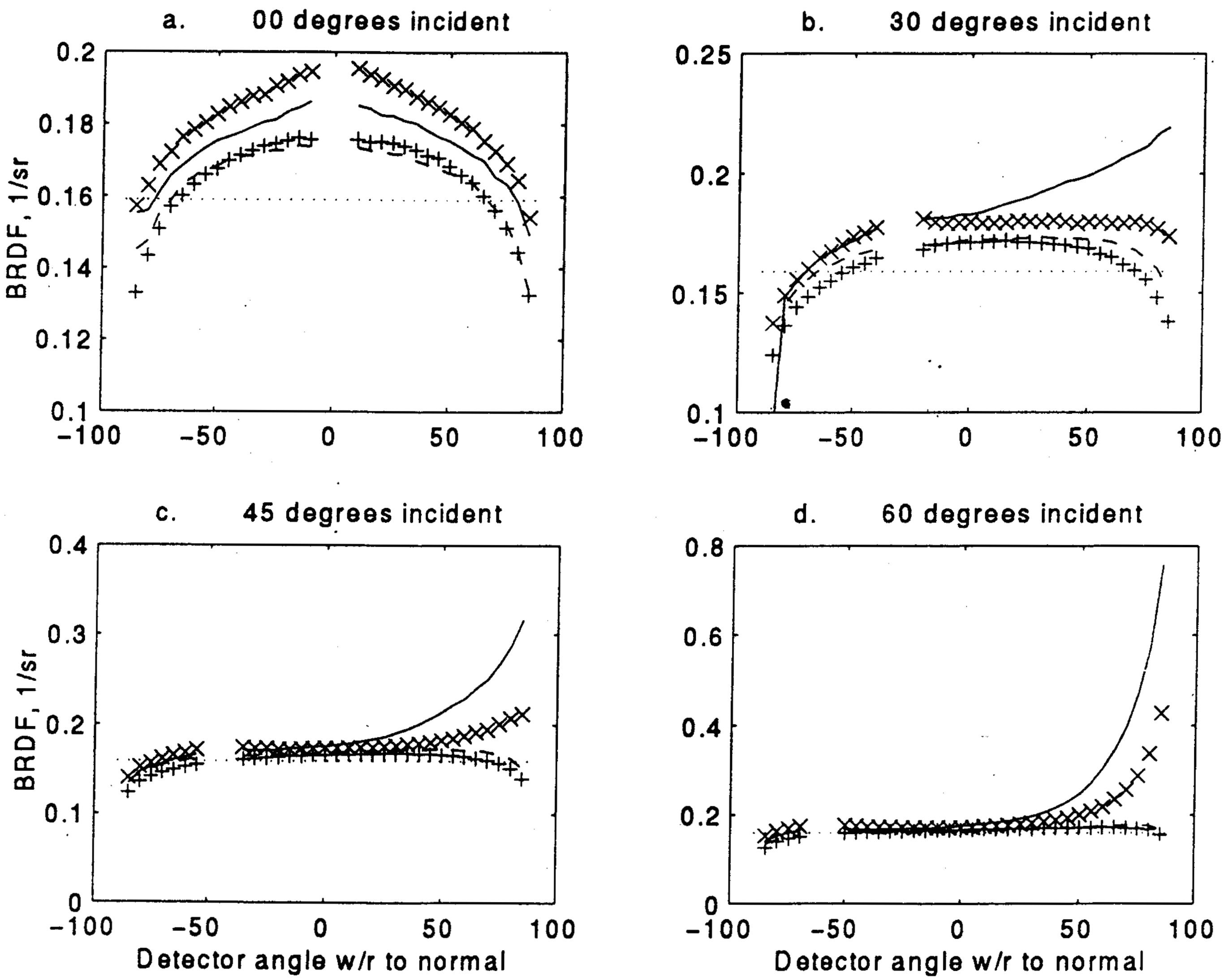

FIGURE 3
HANER

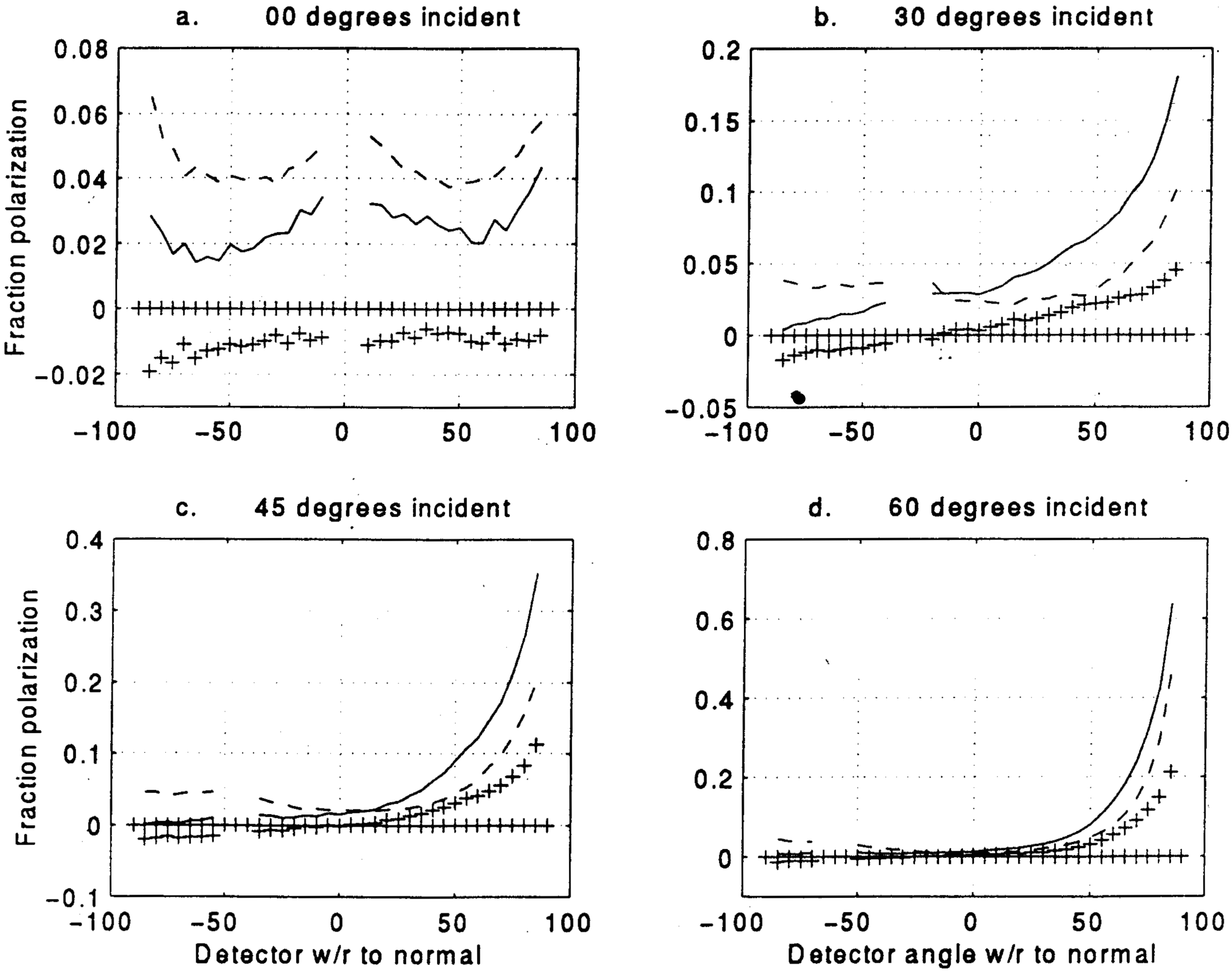

FIGURE 4
HANEL

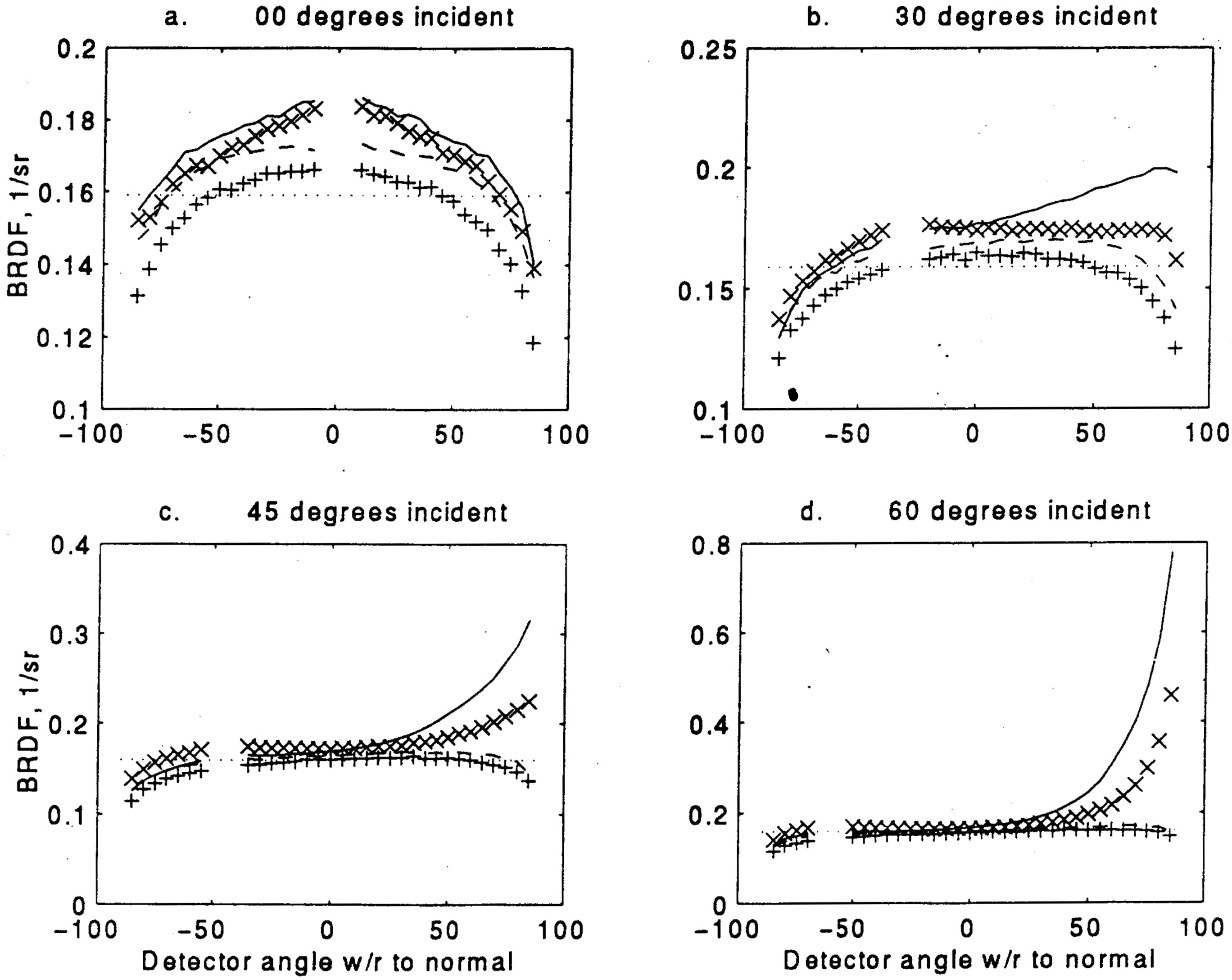

FIGURE 5
HANEK

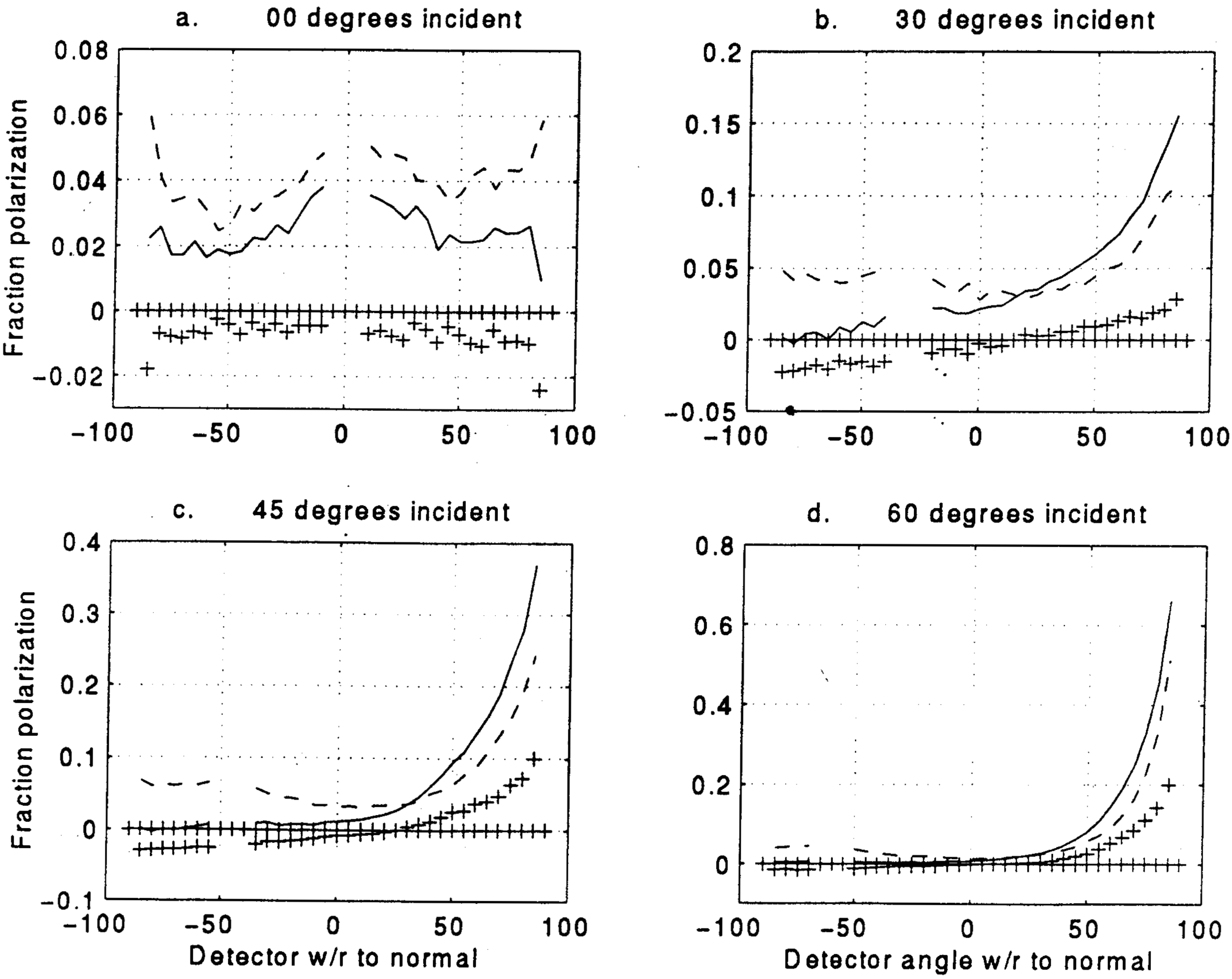

FIGURE 6
HANER

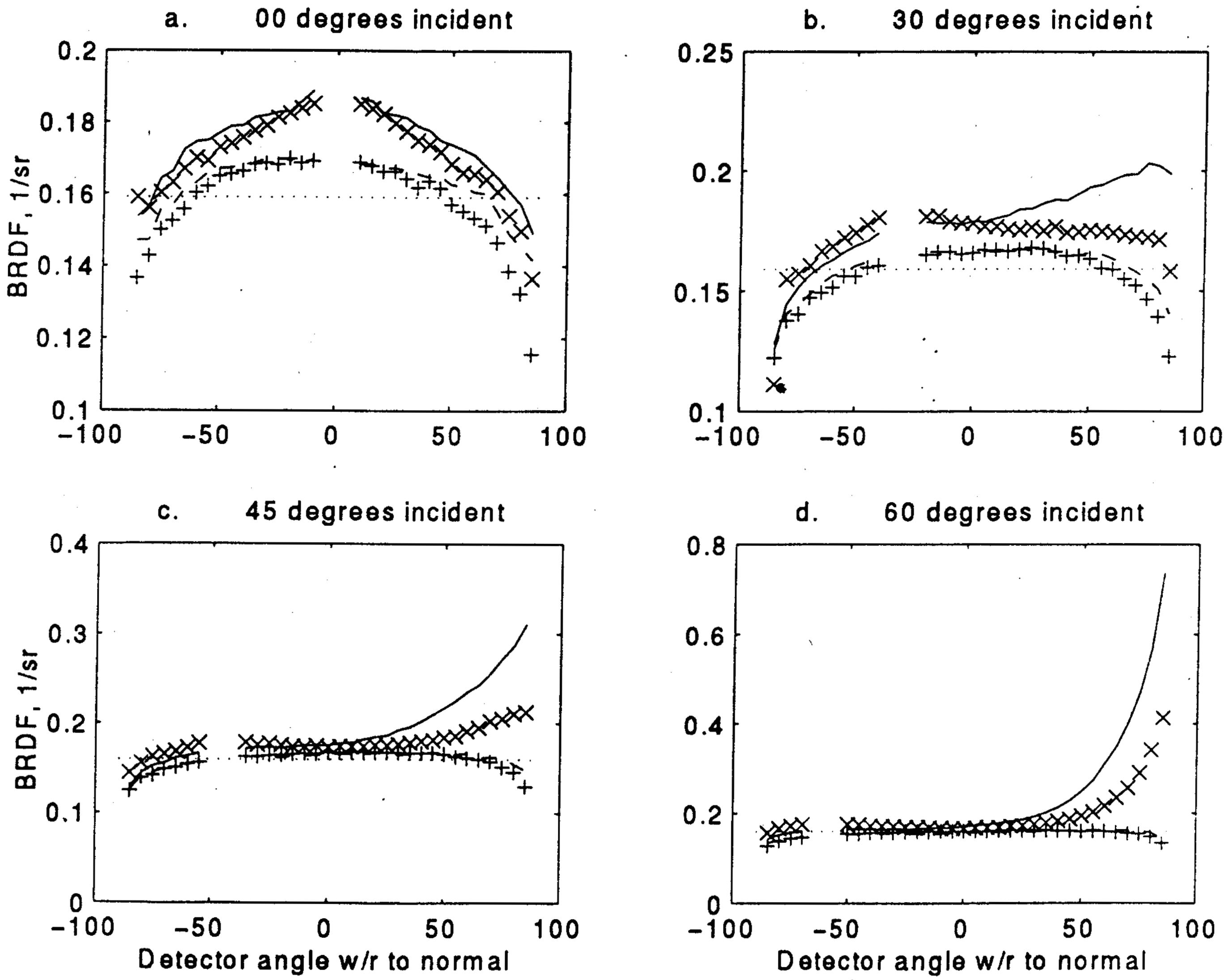

FIGURE 7
HANEK